THE JOURNAL OF BIOLOGICAL CHEMISTRY VOL. 289, NO. 45, pp. 31014–31028, November 7, 2014

Control of Mitochondrial pH by Uncoupling Protein 4 in Astrocytes Promotes Neuronal Survival*

Received for publication, May 2, 2014, and in revised form, September 16, 2014 Published, JBC Papers in Press, September 18, 2014, DOI 10.1074/jbc.M114.570879

Hélène Perreten Lambert[‡], Manuel Zenger[‡], Guillaume Azarias[§], Jean-Yves Chatton[§], Pierre J. Magistretti[‡¶‖], and Sylvain Lengacher[‡‖1]

From the [‡]School of Life Sciences, Brain Mind Institute, Ecole Polytechnique Fédérale de Lausanne, 1015 Lausanne, Switzerland, the [¶]King Abdullah University of Science and Technology, Thuwal 23955-6900, Kingdom of Saudi Arabia, the [§]Department of Fundamental Neurosciences, University of Lausanne, Rue du Bugnon 9, 1005 Lausanne, Switzerland, and the [‖]Center for Psychiatric Neuroscience, 1008 Prilly-Lausanne, Switzerland

Background: The role of uncoupling proteins (UCP) in the brain is unclear.
Results: UCPs, present in astrocytes, mediate the intramitochondrial acidification leading to a decrease in mitochondrial ATP production.
Conclusion: Astrocyte pH regulation promotes ATP synthesis by glycolysis whose final product, lactate, increases neuronal survival.
Significance: We describe a new role for a brain uncoupling protein.

Brain activity is energetically costly and requires a steady and highly regulated flow of energy equivalents between neural cells. It is believed that a substantial share of cerebral glucose, the major source of energy of the brain, will preferentially be metabolized in astrocytes via aerobic glycolysis. The aim of this study was to evaluate whether uncoupling proteins (UCPs), located in the inner membrane of mitochondria, play a role in setting up the metabolic response pattern of astrocytes. UCPs are believed to mediate the transmembrane transfer of protons, resulting in the uncoupling of oxidative phosphorylation from ATP production. UCPs are therefore potentially important regulators of energy fluxes. The main UCP isoforms expressed in the brain are UCP2, UCP4, and UCP5. We examined in particular the role of UCP4 in neuron-astrocyte metabolic coupling and measured a range of functional metabolic parameters including mitochondrial electrical potential and pH, reactive oxygen species production, NAD/NADH ratio, ATP/ADP ratio, CO_2 and lactate production, and oxygen consumption rate. In brief, we found that UCP4 regulates the intramitochondrial pH of astrocytes, which acidifies as a consequence of glutamate uptake, with the main consequence of reducing efficiency of mitochondrial ATP production. The diminished ATP production is effectively compensated by enhancement of glycolysis. This nonoxidative production of energy is not associated with deleterious H_2O_2 production. We show that astrocytes expressing more UCP4 produced more lactate, which is used as an energy source by neurons, and had the ability to enhance neuronal survival.

The uncoupling phenomenon of respiration from ATP production in favor of the production of heat (1) has been well described for the uncoupling protein 1 (UCP1, thermogenin)[2] (2, 3). This phenomenon is controlled by the sympathetic nervous system and is mainly present in specific tissues dedicated to the production of heat, such as brown adipose tissue.

The common term "uncoupling protein" is a legacy of the analysis of sequence homology with UCP1. It is used for other UCP isoforms whose role is less established and not necessarily related to heat production. As far as UCP2 is concerned, its role is related to temperature control (4) and regulation of reactive oxygen species (ROS) (5) in the tissues studied. UCP3 expression correlates with free fatty acid production (6) with a decoupling role primarily in muscle (7); its expression is marginal in brain (8). The role of UCP4 and UCP5 is still largely unknown. In brain, UCP4 and 5 mRNA levels are modulated by diet or temperature changes (9). A role in the regulation of ROS has been described in neural cells (10, 11).

Neurons and astrocytes present different metabolic profiles (12). Neurons are highly oxidative, producing ROS, whereas astrocytes are predominantly glycolytic. In the brain, a role in ROS and temperature control have been described for UCP2 (4). UCP4 and UCP5 are well expressed in the brain (13, 14), and roles in ROS and calcium level regulation (10, 15) have been described. In terms of brain cellular localization, immunocytochemistry has revealed that UCP4 is mainly expressed in neurons and less so in astrocytes (16). UCP5 is present in neuronal cell lines (17, 18); in the rodent brain, UCP5 expression is observed in the dorsomedial hypothalamic nucleus, hippocampus, paraventricular thalamic nucleus, mediodorsal thalamic nucleus, and ventromedial hypothalamus (13, 19).

In summary, only limited information is currently available regarding the role of UCPs in the brain, with the main observations with a cellular resolution being limited to neurons. In this

* This work was supported by Swiss National Science Foundation Grants 108336 (to P. J. M.) and 31003A-135720 (to J. Y. C.).
[1] To whom correspondence should be addressed: School of Life Sciences, Brain and Mind Inst., Ecole Polytechnique Fédérale de Lausanne, 1015 Lausanne, Switzerland. Tel.: 41-21-693-1664; E-mail: Sylvain.Lengacher@epfl.ch.

[2] The abbreviations used are: UCP, uncoupling protein; ROS, reactive oxygen species; OCR, oxygen consumption rate; Tricine, *N*-[2-hydroxy-1,1-bis(hydroxymethyl)ethyl]glycine; MTT, 3-(4,5-dimethylthiazol-2-yl)-2,5-diphenyltetrazolium bromide; Bicine, *N*,*N*-bis(2-hydroxyethyl)-glycine.

study, we have investigated the roles of UCP4 and UCP5 in astrocytes, a cell type central to brain energy metabolism.

We have previously shown (20) that uptake into astrocytes of neuronally released glutamate results in an intramitochondrial pH decrease in astrocytes rapidly reducing the effectiveness of the oxidative phosphorylation. In the present report, we show that this effect of glutamate involves UCP4. Indeed, we observed that the decrease in oxidative efficiency following glutamate uptake into astrocytes is controlled by UCP4, which reduces mitochondrial respiration by lowering the intramitochondrial pH. Reducing mitochondrial efficiency promotes aerobic glycolysis in astrocytes. Lactate produced through glycolysis can be used by neurons as an energy substrate consistent with the astrocyte-neuron lactate shuttle (21). These results indicate that UCP4 plays a key role in astrocyte-neuron metabolic coupling (12).

EXPERIMENTAL PROCEDURES

Primary Culture of Astrocytes—Primary cultures of cortical astrocytes were prepared from newborns (1–2 days old) Swiss Albino mice (OF1; Charles River Laboratories) as previously described (22). The cells were seeded at a density of $\sim 10^5$ cells/cm^2. Depending on the experiments, the cells were seeded on 35-mm Petri dishes or multiwell plates of 6, 12, 24, or 48 wells. The plates were incubated at 37 °C in an atmosphere containing 5% CO_2 and 95% air. The cells were rinsed 3–5 days after seeding, and the medium was changed twice a week until cells reached confluency at 21 days *in vitro*. Experiments were performed on confluent cells.

Primary Cultures of Neurons and Co-culture—Primary cultures of cortical neurons were prepared from embryonic day 17 OF1 mice embryos (Charles River Laboratories). Pregnant mice were sacrificed by cervical dislocation. The abdomen was opened, and the placenta containing the embryos was removed and put in a Petri dish. The embryos were rapidly recovered, and the cut heads were placed in Petri dish containing 25 ml of ice-cold Hanks' buffered salt solution supplemented with penicillin and streptomycin. The embryo brains were separated from the skulls, and olfactory bulbs, striata, hippocampi, and meninges were removed. The isolated cortices were minced in 2-mm^2 pieces and incubated at 37 °C for 30 min in a solution containing papain 20 units/ml (Worthington Biochemical), 1 mM L-cysteine, 0.5 mM EDTA, and 100 units/ml DNase (Worthington Biochemical). Papain activity was then inhibited by addition of FCS. Any traces of papain were removed by keeping the cells sedimenting and removing the supernatant. Cell pellet was resuspended in Neurobasal medium (21103049; Invitrogen) supplemented with penicillin-streptomycin, B27 (17504044; Invitrogen), and GlutaMAX (35050038; Invitrogen), and single-cell suspension was obtained by repeated mechanical trituration. The cellular debris was removed by centrifugation at 200 × *g* for 5 min. The supernatant was discarded, and the cell pellet was carefully resuspended in prewarmed 5 ml supplemented Neurobasal medium. Cells were plated at an average density of 5×10^4 cells/cm^2 on 20-mm diameter glass coverslips previously coated overnight with 25 mg/liter polyornithine and rinsed three times with sterile water the day of dissection. Neurons were maintained at 37 °C in a humidified atmosphere containing 5% CO_2 and 95% air and were used at day *in vitro* 14. At 21 days, when astrocytes were confluent, medium was exchanged for Neurobasal medium supplemented with GlutaMAX and B27 without antioxidant (B27 minus AO) (10889038; Invitrogen). 24 h later, the co-culture was initiated by transferring 12-day-old neurons grown on coverslips on top of the astrocyte layer culture. The coverslips with neurons were placed in such a way that neurons were facing astrocytes separated by a 3-mm gap created by three paraffin beads attached to the coverslip. The small gap created by the three paraffin beads was sufficient to avoid any contact between the two cell types, and thus to avoid astrocytic contamination of the neuronal culture, but allowed the exchange of medium. Viability experiments were performed 48 h later.

Quantitative Polymerase Chain Reaction—RNA extraction was performed with the RNeasy mini kit from Qiagen as indicated in the manufacturer's instruction. RT reactions were done with the High Capacity RNA-to-cDNA kit (Life Technologies) as indicated in the manufacturer's instructions. Each reaction was done in 20 μl with 400 ng of RNA. Quantitative determination of mRNA of the five uncoupling protein isoforms were performed with the fast real time PCR system 7900HT (Applied Biosystems, Rotkreuz, Switzerland). The following primers were used: mUCP1Fo519, 5′-CGA CTC AGT CCA AGA GTA CTT CTC TTC; mUCP1Re591, 5′-TCC CCT GTT GAT GTG GTC AA; mUCP2Fo992, 5′-TCC CCT GTT GAT GTG GTC AA; mUCP2Re1062, 5′-CAG TGA CCT GCG CTG TGG TA; mUCP3Fo78, 5′-CCT ACG ACA TCA TCA AGG AGA AGT T; mUCP3Re863, 5′-TCC AAA GGC AGA GAC AAA GTG A; mUCP4Fo13, 5′-GAA TGC CTA TCG CCG AGG A; mUCP4Re85, 5′-AGT AGG AAC TTG CTC GTC CGG; mUCP5Fo602, 5′-TCC CAA CTG CTC AGC GTG; mUCP5Re673, 5′-GGT GCT TCT TGG TAA TA TCA TAA ACG; mActinβFo31, 5′-GCT TCT TTG CAG CTC CTT CGT; mActinβRe94, 5′-ATA TCG TCA TCC ATG GCG AAC; mTBPFo271, 5′-ACC TTA TGC TCA GGG CTT GGC C; and mTBPRe359, 5′-GTC CTG TGC CGT AAG GCA TCA TTG.

All primers pairs were designed to overlap exon-exon junction to avoid contamination signal from eventual genomic DNA. Genes for β-actin and TATA box binding protein were used as reference genes for the normalization. The Power SYBR Green (Applied Biosystems) was used as a *Taq* polymerase master mix. All samples were analyzed in triplicate. The results were analyzed with the SDS2.3 software (Applied Biosystems). To compare the expression difference, we first convert the cycle threshold (C_T) in copies number by applying the rule that $C_T = 10$ is equivalent to 1E11 copies and $C_T = 37.34$ is equivalent to 625 copies. We then calculate a normalization value for each sample of the reference genes by dividing each absolute value by the geomean calculated for each reference gene. We obtain a normalization factor for each gene used as calibrator (β-actin, TATA box binding protein). To obtain a calibrator number, we calculated the geomean from these reference numbers. We divided each absolute value obtained for the different samples by this final calibrator number. The result is a normalized value of gene expression for the different UCPs that keep the differences of expression between the various UCPs intact.

Lentiviral DNA Constructs—mRNA for UCP4 and UCP5 were isolated from brain of OF1 mice. Reverse transcription was prepared by using 200 ng of extracted mRNA in 50 μl of total RT. Specific cDNA was obtained by PCR with the following primers: mUCP4FoEcoRI, 5′-GAA TTC TGC TGA ATG CCT ATC GCC; mUCP4ReSphI, 5′-GCA TGC ATG GGC TGA CTC CAC TC; mUCP5FoEcoRI, 5′-GAA TTC GTG AAT GGG TAT CTT TCC; and mUCP5ReXhoI, 5′-CTC GAG GAT CTG AAG CCT CTT GA.

PCR products were cloned in the pGEMT vector (Promega), and UCPs genes were isolated by restriction digestion with EcoRI and SphI for UCP4 and with EcoRI and XhoI for UCP5 and were cloned in the pIRES-hrGFP-2a vector (Stratagene). The gene of interest is thus fused to three contiguous copies of the HA epitope (AGC GTA GTC AGG TAC ATC GTA AGG GTA AGC GTA ATC CGG AAC GTC GTA CGG ATA CGC GTA GTC TGG AAC GTC ATA TGG GTA). The next step in the lentiviral construction is the use of the Gateway System. UCP-HA genes were amplified from the pIRES-hrGFP-2a vector by PCR using the following primers: mUCP4FoTopo, 5′-CAC CAT GGG ACC TAT CGC CGA GGA GGA GAA; mUCP5FoTopo, 5′-CAC CAT GGG TAT CTT TCC CGG AAT AAT CC; and mUCPsReTopo, 5′-ATC TTG TTA AGC GTA GTC AGG TAC ATC GTA AG.

PCRs were performed with a proof reading polymerase (*Pfu* polymerase), and the blunt end PCR products were directly cloned in the pENTR/D-TOPO using the pENTR/D-TOPO cloning kit (Invitrogen). Transfer into the lentiviral vector SIN-PGK-CassRFA-WHV (kindly provided by Dr. H. Hirling, Lausanne, Switzerland) was performed with the Gateway LR Clonase II enzyme mix (Invitrogen) according to the manufacturer's protocol. The lentiviral vectors sequences for silencing UCP4 and UCP5 were purchased from Open Biosystems (reference number for UCP4, RMM3981-97057374, reference number for UCP5, RMM3981-97057464).

Lentivirus Production—HEK 293T cells were transfected with 13 μg of pCMVΔ8.92, 3 μg of pRSV-ReV, 3.75 μg of pMD2G, and 13 μg of the vector SIN-PGK-WHV containing the transgene per Petri dish with the calcium phosphate method and maintained at 37 °C in a humidified atmosphere containing 5% CO_2 and 95% air. Medium was replaced 6–8 h later. Medium containing lentiviruses were collected 3 days after transfection, filtered at 0.45 μm (Stericup SCHVU01RE; Millipore), and spun at 19000 rpm for 90 min at 4 °C in an ultracentrifuge using SW32Ti rotors (BD Biosciences). The supernatants were removed, and each pellet containing viruses was suspended in PBS, 0.5% BSA and frozen at −80 °C. Viral titration was determined using the HIV-1 P24 ELISA kit (Zeptometrix Corporation, Buffalo, NY) as indicated in the manufacturer's instructions. For UCP overexpression, astrocytes were infected from days 3 to 5 *in vitro* with a final concentration of 400 ng of p24 per 35-mm Petri dish. As a control, we infected astrocytes with a lentivirus coding for GFP. The UCP expression was similar to noninfected astrocytes (data not shown), suggesting that the infection itself had no effect on UCP gene expression. For gene silencing, astrocytes were infected at a final concentration of 100 ng of p24 per 35-mm Petri dish. The mature antisense coded by the shUCP4 virus was AAT ATT GGG TAT CCA GCC TGC. The mature antisense coded by the shUCP5 virus was ATT TCT TTG AAA CGA ACA TCG. As a control of gene silencing, we infected astrocytes with a lentivirus made with a vector containing no sequence.

Western Blots—When astrocytes reached confluency at day 21 *in vitro*, 35-mm Petri dishes of infected cells were placed on ice and rinsed with ice-cold PBS. Cells were homogenized and proteins were extracted with 200 μl/dish of lysis buffer (30 mM HEPES, 210 mM sucrose, 40 mM NaCl, 2 mM EDTA, 1% SDS, and a mixture of protease inhibitors (Complete 11257000; Roche). Each condition was made in duplicate, and two dishes were mixed. Protein samples were sonicated and frozen at −80 °C. 10 μl of each samples were mixed to 10 μl of 2× loading buffer (100 mM Tris-Cl, pH 6.8, 200 mM DTT, 4% SDS, 0.1% bromphenol blue, 10% glycerol) and heated at 100 °C for 4 min before loading onto an Invitrogen NuPage 10% gel (NP0301BOX). When proteins were loaded after mitochondrial isolation following the mitochondria isolation kit (MITOISO1; Sigma-Aldrich) protocol, 2.5 μg of protein were loaded. Gel was run at 100 volts at 4 °C. After running, proteins were transferred on nitrocellulose membranes (84261514; Whatman) in a Tris-glycine transfer buffer (0.4 M glycine, 0.25 M Tris-base, pH 6.8, 20% methanol). Transfers were done by application of 75 volts for 80 min at 4 °C. Membranes were incubated for 1 h in the Odyssey blocking buffer (927-40000; LI-COR) at room temperature and then incubated overnight at 4 °C with primary antibodies polyclonal anti-HA (1:4000) (AB9110; Abcam), monoclonal anti-β actin (1:5000) (A5441; Sigma-Aldrich), or monoclonal anti-cytochrome *c* oxidase (1:1000) (MS407; Mitosciences) diluted in the same blocking buffer. After several washes in PBS, secondary antibodies anti-mouse IgG IRDye 800 (1:5000) (610-132-121; Bioconcept) and anti-rabbit IgG Alexafluor 680 (1:5000) (Juro, Lucerne, Switzerland) were applied for 2 h at room temperature and protected from light. After washing, membranes were scanned with the ODYSSEY Infrared Imaging System (LI-COR Biosciences).

Immunocytochemistry—Astrocytes grown on 20-mm coverslips and infected with UCP lentiviral constructs were carefully rinsed with PBS before being fixed in cold paraformaldehyde 4% for 15 min at room temperature. Treatment with PBS, 0.1% Triton for 15 min was performed to permeabilize the cell membranes. After three PBS washes, fixed cells were then treated with casein (0.5% in PBS) for 1 h at room temperature to block nonspecific sites. Fixed cultures were then incubated overnight at 4 °C in the presence of the primary antibodies polyclonal anti-HA (1:500) (AB9110; Abcam), polyclonal GFAP (1:500) (Z0334; Dako), or monoclonal anti-cytochrome *c* oxidase (1:500) (MS407; Mitosciences). After three repeated washes in PBS, cells were incubated in the secondary antibodies goat anti-rabbit Alexa 488 (1:200) (A11008; Invitrogen) and goat anti-mouse Alexa 594 (1:200) (A11005; Invitrogen) for 2 h at room temperature in the dark. After rinsing, coverslips were mounted in a solution containing 50% glycerol and DABCO (D2522; Sigma-Aldrich) to reduce photobleaching. Z-stack acquisitions were done using a confocal microscope ZEISS LSM 710. The images underwent deconvolution using Huygens Remote Manager v1.2.2 and were then analyzed using the Imaris Software (Bitplane Corp.). Co-localization between UCP

and mitochondria was calculated with the Manders' coefficient which is the part of the intensity in each channel that coincides with a number of intensity in the other channel (with 0 indicating no co-localization and 1 indicating perfect co-localization).

Glucose Uptake Assay—Glucose uptake was measured as previously described (23). The effect of glutamate on astrocytic glucose uptake was measured in parallel in other Petri dishes by adding glutamate 200 μM in the medium containing [^{3}H]2-deoxyglucose for 20 min of incubation. Other Petri dishes were used to measure the portion of glucose uptake that is not linked to glucose transporter by addition of the glucose transporter inhibitor cytochalasin B (C6762; Sigma-Aldrich) 25 μM during 20 min of incubation. The fraction of glucose transported is calculated by subtracting the fraction of glucose uptake that is not inhibited by the cytochalasin B. Glucose uptake was normalized to the protein content.

Glycogen Content—Glycogen content was measured enzymatically as previously described (22). In brief, astrocytes grown on 35-mm Petri dishes and previously infected with UCP lentiviral constructs were washed three times with ice-cold PBS and lysed by sonication in HCl 30 mM. Two aliquots of 100 μl were sampled. 300 μl of 0.1 M acetate buffer, pH 4.65, was added to the first aliquot, whereas the same buffer containing 1% amyloglucosidase (10 mg/ml) was added to the other one. After incubation at room temperature for 30 min, 2 ml of 0.1 M Tris-HCl buffer, pH 8.1, containing 3.3 mM $MgCl_2$, 0.33 mM ATP, 38 μM NADP, 4 μg/ml hexokinase, and 2 μg/ml glucose-6-phosphate dehydrogenase were added, and the mixture was incubated at room temperature for 30 min. Fluorescence associated with the formation of NADPH was read on a fluorometer using excitation wavelength at 340 nm and emission wavelength at 450 nm. Glycogen was normalized to protein content and was expressed as glycosyl units originating from glycogen. The results are expressed as percentages of control values.

Mitochondrial Potential Measurement—Astrocytes grown on a multiplate of 48 wells and previously infected with UCP lentiviral constructs were rinsed carefully and incubated 1 h in phenol red-free DMEM (D5030; Sigma) supplemented with 2 mM glucose and 44 mM $NaHCO_3$. After rinsing, cells were incubated in the same medium containing 5 μg/ml JC-1 dye (T-3168; Invitrogen) for 30 min at 37 °C in an atmosphere containing 5% CO_2 and 95% air and protected from light. The JC-1 dye exhibits potential dependent accumulation in mitochondria, indicated by a fluorescence emission shift from green to red (24, 25). At low potential, monomers are formed that display green fluorescence, whereas at higher potential, JC-1 aggregates and exhibits a red fluorescence. Cells were carefully rinsed with PBS to remove any extracellular dye, and fluorescence was directly detected on the multiplate using a fluorometer (Safir 2; Tecan). The wavelengths used are emission 497/excitation 594 for the red fluorescence and emission 497/excitation 524 for the green fluorescence. The mitochondrial potential was estimated by calculating the ratio of green to red fluorescence. The results are expressed as percentages of control values.

ATP/ADP Ratio—ATP content was measured enzymatically with the luciferase. In the presence of ATP, Mg^{2+}, and oxygen, luciferin is oxygenated by luciferase into oxyluciferin. This reaction emits light that is proportional to the amount of ATP. ATP was determined with the CellTiter-Glo Luminescent cell viability assay (Promega) with some modifications. Astrocytes grown on multiplate of 48 wells and previously infected were rinsed and incubated 1 h at 37 °C in an atmosphere containing 5% CO_2 and 95% air in DMEM (D5030; Sigma-Aldrich) containing 44 mM $NaHCO_3$ and 2 mM glucose. At the end of the incubation, medium was removed, and 200 μl of Tricine buffer solution (40 mM Tricine, 3 mM EDTA, 85 mM NaCl, 3.6 mM KCl, 100 mM NaF, and 0.1% saponin (84510; Sigma-Aldrich), pH 7.4) was put in each well. Cells were lysed by saponin effect and by pipetting. The saponin is a "soft" soap that breaks cell membranes but preserves the enzymatic reaction. Each sample was separated in two: one part for ATP measure and the other part for ATP + ADP measure. 90-μl aliquots were distributed in a black-walled 96-well type microplates (PerkinElmer Life Sciences). For the ATP + ADP measure, 10 μl of converting solution (100 mM Tricine, 100 mM $MgSO_4$, 25 mM KCl, 1 mM phosphoenolpyruvate, and 100 units/ml pyruvate kinase), pH 7.75, was added in each well, whereas the same solution without phosphoenolpyruvate and pyruvate kinase was added to the samples for ATP measure. An incubation of 5 min at room temperature was performed before adding 10 μl of $MgCl_2$ solution (4 mM Tricine and 100 mM $MgCl_2$). Finally, 100 μl of CellTiter-Glo reagent (G7571; Promega) was added, and luminescence was immediately detected with a luminometer (Safire 2; Tecan). Luminescence was measured in a kinetic way determined by 20 readings at intervals of 1 min. Luminescence read at the plateau were taken to calculate the ATP/ADP ratio. ADP values were calculated by subtracting ATP values from ATP + ADP values. The results are expressed as percentages of control values.

Hydrogen Peroxide Quantification—H_2O_2 accumulated in the medium and was detected enzymatically with Amplex red (26, 27). Oxidation of Amplex red is catalyzed by the horseradish peroxidase in the presence of H_2O_2 into highly fluorescent resorufin. When reaching confluency, astrocytes grown on multiplates of 24 wells and previously infected with UCP lentiviral constructs were carefully rinsed before being incubated 4 h in phenol red free Neurobasal medium supplemented with GlutaMAX and B27 without antioxidant (B27 minus AO) and containing 10 μM Amplex red (A12222; Invitrogen) and 1 unit/ml horseradish peroxidase (type II, P8250; Sigma-Aldrich). At the end of the incubation, 100 μl were loaded on a black-walled 96-well plate (PerkinElmer Life Sciences), and fluorescence was detected using wavelengths at 545 nm for excitation and 590 nm for emission. The results are expressed as percentages of control values.

NAD^+/NADH Cycling Assay—NADH and NAD^+ were measured enzymatically as previously described (28) with some modifications. NAD^+ is reduced by alcohol dehydrogenase in the presence of ethanol. NAD^+ is renewed by the reduction of phenazine ethosulfate, whose oxidized form is restored by the reduction of MTT. Reduced MTT is visualized by absorbance at 570 nm. Infected astrocytes grown on 35-mm Petri dish and reaching confluency were incubated 24 h in phenol red-free Neurobasal medium without glucose (0050128DJ; Invitrogen) supplemented with 5 mM glucose, B27, and GlutaMAX. The

cells were then put on ice and washed three times with ice-cold PBS. Cells were recovered in 600 μl of carbonate-bicarbonate (20 mM to 100 mM) buffer, pH 10, containing 10 mM nicotinamide (72340; Sigma-Aldrich) and were directly frozen to disrupt cell membrane. Once thawed, the samples were kept on ice and separated in two parts: one for the dosage of NADH + NAD^+ and the other for NADH only. Samples for NADH detection were heated at 60 °C for 30 min to destroy NAD^+ and were kept on ice. 50 μl of each samples were loaded on a 96-well microplate, and the reaction was initiated by addition of 150 μl of reaction mix composed of 133 mM Bicine (14871; Sigma-Aldrich), 5.33 mM EDTA, 0.56 mM MTT (M5655; Sigma-Aldrich), 2.21 mM phenazine ethosulfate (0210095601; MP Biomedicals), 667 mM ethanol, and 40 units/ml alcohol dehydrogenase (A3263; Sigma-Aldrich). Reduction of MTT was followed by measuring absorbance at 570-mm 30 times at intervals of 30 s. NAD^+ values were calculated by subtracting NADH from NADH + NAD^+ values. Concentrations were determined from a standard curve from 0.1 to 2 μM NADH (10107735001; Roche) and were normalized to the protein content. the results are expressed as percentages of control conditions.

CO_2 Production Assay—CO_2 production was measured by incorporation of radioactive labeled glucose as previously described (29). This technique enabled us to distinguish the quantity of CO_2 produced by glucose metabolism via the TCA cycle between those produced by the pentose phosphate pathway. D-[1-^{14}C]Glucose produces $^{14}CO_2$ via the two pathways, whereas $^{14}CO_2$ produced by D-[6-^{14}C]glucose is exclusively provided by the TCA cycle. CO_2 produced specifically by the TCA cycle is determined by metabolization of D-[6-^{14}C]glucose, whereas use of D-[1-^{14}C]glucose gives the total amount of CO_2 formed. When reaching confluency, medium of astrocytes growing on 35-mm Petri dishes was changed for DMEM (D5030; Sigma-Aldrich) containing 2.5 mM glucose, 7.5 mM $NaHCO_3$, 5 mM HEPES, and 10 ml/liter antibiotic/antimycotic solution, and cells were incubated 2 h at 37 °C in an atmosphere containing 5% CO_2 and 95% air. The medium was then replaced by 1 ml of the same medium supplemented with 2.3 μCi/ml D-[1-^{14}C] (CFA349; Amersham Biosciences) glucose or D-[6-^{14}C]glucose (CFA351; Amersham Biosciences), and culture dishes were placed in sealed glass containers and incubated for 2 h at 37 °C. 0.2 M HCl was injected in dishes containing the respiring cells to stop the reaction, and radioactive $^{14}CO_2$ was captured by addition of 1 ml of Carbo-Sorb (PerkinElmer Life Sciences) against the walls of the container. These were kept aside 1 h for equilibration, and two aliquots of 400 μl of Carbo-Sorb were taken for radioactivity assay by liquid scintillation counting (Permafluor E^+; PerkinElmer Life Sciences). The values were normalized to the protein content, and the results are expressed as percentages of control values.

Oxygen Consumption Rate—The oxygen consumption rate (OCR) was assessed using a noninvasive extracellular flux analyzer (XF24; Seahorse Biosciences, North Billerica, MA). It is composed of two calibrated optical sensors that directly measure the oxygen consumption rate in a 7-μl microchamber with limited diffusion. The depletion of oxygen in the medium is then measured several times during a defined period. Injector ports surrounding the sensor of each well can be used to automatically deliver drugs during the experiment. The cells were plated in XF24 wells (XF24 FluxPaks, 100850-001; Bucher, Basel, Switzerland) of 0.38 cm^2 area per well and incubated for 1 h in a non-CO_2 incubator with unbuffered medium before loaded in the XF24 Analyzer. For astrocytes, the medium was composed of DMEM (D5030; Sigma-Aldrich) supplemented with 32 mM NaCl, 15 mg/liter Phenol red, 10 mM 2-deoxyglucose, 5 mM glucose, and 5 mM pyruvate. For neuronal cultures, medium was composed of DMEM supplemented with 32 mM NaCl, 15 mg/liter Phenol red, and 0.5 mM glucose. During the measure, 200 μM glutamate was first added in astrocytes culture. In neurons, glucose and/or lactate were injected at energetically equivalent concentrations as indicated. In all cases, later injection of 5 μM oligomycin (75352; Sigma-Aldrich) and 2 μM carbonyl cyanide-4-(trifluoromethoxy)phenylhydrazone (C2920; Sigma-Aldrich) provided estimation of the success of the experiment. Effect of glutamate was normalized to the basal OCR, as well as the effect of glucose and/or lactate in neurons. The results are expressed as percentages of control values.

Mitochondrial Matrix pH—Two-week-old astrocytes were placed in 2 ml of antibiotic-free and serum-free DMEM with FuGENE (Roche) and DNA encoding for genetically encoded pH indicator MitoSypHer (30). Quantities of DNA/FuGENE were 2 μg of DNA/12 μl of FuGENE for MitoSypHer and 4 μg of DNA/8 μl of FuGENE for MIMS-EYFP. After 4 h, the medium was changed with DMEM plus 10% serum, and the cells were used 2–3 days after transfection for pure astrocyte culture and 14 days for mixed neuron-astrocyte cultures. Mitochondrial matrix pH was measured by fluorescence microscopy as previously described (20). Briefly, cells were placed in a thermostatted chamber designed for rapid exchange of perfusion solutions (31) and superfused at 35 °C. Experimental solution contained 160 mM NaCl, 5.4 mM KCl, 20 mM HEPES, 1.3 mM $CaCl_2$, 0.8 mM $MgSO_4$, 0.78 mM NaH_2PO_4, 5 mM glucose (pH 7.4) and was bubbled with air. MitoSypHer fluorescence was sequentially excited at 490 and 420 nm and detected at >515 nm. At the end of each experiment, *in situ* calibration was performed by permeabilization of cells with 10 μM monensin and 3 μM gramicidin and superfused with a series of calibration solutions of given pH values (pH 5.9, 7.0 7.5, and 8.0). Calibration solutions contained 20 mM NaCl, 125 mM KCl, 0.5 mM $MgCl_2$, 0.2 mM EGTA, 20 mM HEPES and bubbled with air.

Lactate Release Assay—Lactate released by astrocytes previously infected with UCP lentiviral constructs was determined with an enzymatic method, first described by Rosenberg and Rush (32) with some modifications. Lactate dehydrogenase oxidizes lactate into pyruvate in the presence of NAD^+. The resulting NADH is measured by fluorometry. 24 h after co-culture initiation, 10 μl of medium was taken and mixed with 190 μl of medium. This was mixed with 1 ml of 0.2 M glycine-semicarbazide, pH 10 buffer containing 2 mg/ml NAD and 13.75 units/ml lactate dehydrogenase and was incubated at 40 °C for 1 h. 200 μl of this reaction was transferred into a black-walled 96-well plate (PerkinElmer Life Sciences). The formation of NADH was measured by fluorescence (Safire 2; Tecan) using excitation wavelength at 340 nm and emission wavelength at 450 nm. Absolute values were determined from a standard curve, and

lactate release in the medium was normalized to the DNA quantity in each Petri dish using the PicoGreen method. For this normalization, cells were incubated for 5 min in PBS containing PicoGreen solution (P7589; Invitrogen) diluted 1:200. After washing, fluorescence was measured using excitation wavelength at 480 nm and emission wavelength at 520 nm. The results are expressed as percentages of control values.

Viability Test: Calcein Assay—48 h after co-culture initiation, coverslips with neurons were transferred to new wells containing Neurobasal medium supplemented with GlutaMAX, B27 without antioxidant (B27 minus AO), and 1 μg/ml calcein-AM. Neurons were carefully rinsed, and calcein fluorescence was measured directly in the multiwell plate with a fluorescence reader (Safire 2; Tecan) with excitation wavelength of 490 nm and emission of 515 nm. The calcein fluorescence was normalized to the cell quantity in each well by adding the nucleus marker DAPI (D9542; Sigma-Aldrich). Neurons were incubated for 10 min in PBS containing DAPI 7 μg/ml, and after rinsing, DAPI fluorescence was measured using excitation wavelength at 360 nm and emission at 461 nm. The results are expressed as percentages of control values.

Viability Test: MTT Reduction Assay—Viability of neurons in co-culture were measured with the MTT (M5655; Sigma-Aldrich) reduction assay (33). 48 h after co-culture initiation, MTT was directly put into the co-culture medium to a final concentration of 0.2 mg/ml, and cells were incubated 30 min at 37 °C in an atmosphere containing 5% CO_2 and 95% air. At the end of the incubation, neuronal coverslips were transferred to new wells containing 500 μl of DMSO to stop the reaction of dehydrogenases. The amount of reduced MTT (formazan) solubilized in DMSO was then determined spectrophotometrically using absorbance at 560 nm (Safire 2; Tecan). The values were normalized to the DNA quantity in each well. For this normalization, the cells were incubated for 5 min in PBS containing PicoGreen solution (P7589; Invitrogen) diluted 1:200. After washing, fluorescence was measured using excitation wavelength at 480 nm and emission wavelength at 520 nm. The results are expressed as percentages of control values.

Mitochondrial Mass Determination—To determine mitochondrial mass in astrocytes or neurons, we used Mitotracker Red FM (M-22425; Invitrogen). Cells in culture were rinsed with prewarm PBS before incubation in DMEM (D5030; Sigma-Aldrich) supplemented with 2 mM glucose, 44 mM $NaHCO_3$, and 20 nM Mitotracker Red 580 (M-22425; Invitrogen) for 20 min at 37 °C. The cells were rinsed with PBS, and fluorescence was measured using excitation wavelength at 581 nm and emission wavelength at 664 nm. The values were then normalized to the DNA quantity in each well using the PicoGreen as described above for the MTT measurement.

Statistics—All results are presented as the means ± S.E. The data were analyzed for statistical significance against respective controls by analyze of variance with multiple comparisons using Dunnett's post hoc test. *, **, and *** refer to p values <0.05, 0.01, and 0.001, respectively. The software used was Instat 3.0 software (GraphPad, San Diego, CA).

TABLE 1

Quantitative PCR levels of the different UCPs isoforms in astrocytes and neurons mouse primary cultures

To assess real differences level of mRNA for the various UCPs isoforms, we convert quantitative PCR data in copy number. To evaluate the differences between the different UCP isoforms, we have arbitrary set the UCP4 copy number to 100. The other UCPs isoforms are shown as percentages compared with astrocyte UCP4 expression level. This representation highlights the differences of each UCP isoform between astrocytes and neurons expression levels.

	UCP1	UCP2	UCP3	UCP4	UCP5
Astrocytes	0.33 ± 0.02	183 ± 3	0.08 ± 0.02	100 ± 2	291 ± 12
Neurons	1.72 ± 0.27	119 ± 45	0.06 ± 0.02	321 ± 35	478 ± 32

RESULTS

Mitochondrial Localization of Overexpressed UCPs in Astrocytes—Expression of various UCPs in the brain has been previously reported (8, 34). The results presented in Table 1 summarize the expression levels for each UCPs isoform in astrocyte and in neuron mouse primary cultures. UCP2, UCP4, and UCP5 are the main UCP isoforms and are expressed both in astrocytes and neurons.

Overexpression of the various isoforms of uncoupling protein in primary cultures of astrocytes through viral transfection results in an increased expression of the corresponding UCP isoform as determined by RT-PCR. The increase ranged from a 250-fold increase in mRNA for UCP2, UCP4, and UCP5 to 30,000-fold for UCP1 and UCP3 (one should note that the expression levels of these two latter isoforms were extremely low before transfection). Using silencing constructs for UCP4 or UCP5 (see "Experimental Procedures"), we observed a reduction in the corresponding UCPs mRNAs (data not shown).

We also analyzed the expression and the subcellular localization of overexpressed uncoupling proteins by Western blotting and immunohistochemistry. For increased specificity, we used an hemagglutinin epitope (HA tag) (see "Experimental Procedures") fused to UCP sequences that allows us to determine the expression of each overexpressed isoform. As seen in Fig. 1*A*, all isoforms are present in astrocytes infected with the corresponding UCP construct, detected by a band close to 32 kDa. For the UCP5 protein, two bands were observed in some blots, most likely resulting from alternative splicing (9).

UCP4 and UCP5 overexpression was also determined in mitochondrial preparations. Mitochondrial fraction was separated from cytosolic fraction and run on a polyacrylamide gel. Antibody against cytochrome oxidase was used as a marker of the mitochondrial fraction. Uncoupling proteins 4 and 5 were highly enriched in the purified mitochondrial fraction (Fig. 1*B*). Mitochondrial localization of the overexpressed uncoupling proteins was also confirmed by immunohistochemistry in astrocytes. Primary antibodies directed against the HA tag and the mitochondrial cytochrome oxidase were used for co-localization analysis. The UCP4-HA (Fig. 1*C*) is revealed in *green*, whereas cytochrome oxidase is revealed in *red*, and co-localization appears in *white*. The results in Fig. 1*C* showed that UCP4-HA co-localized with the cytochrome oxidase, suggesting that the overexpressed uncoupling protein was targeted to the mitochondria.

We tested the viability of the lentivirus-infected astrocytes using the calcein test and found that it did not affect cell survival

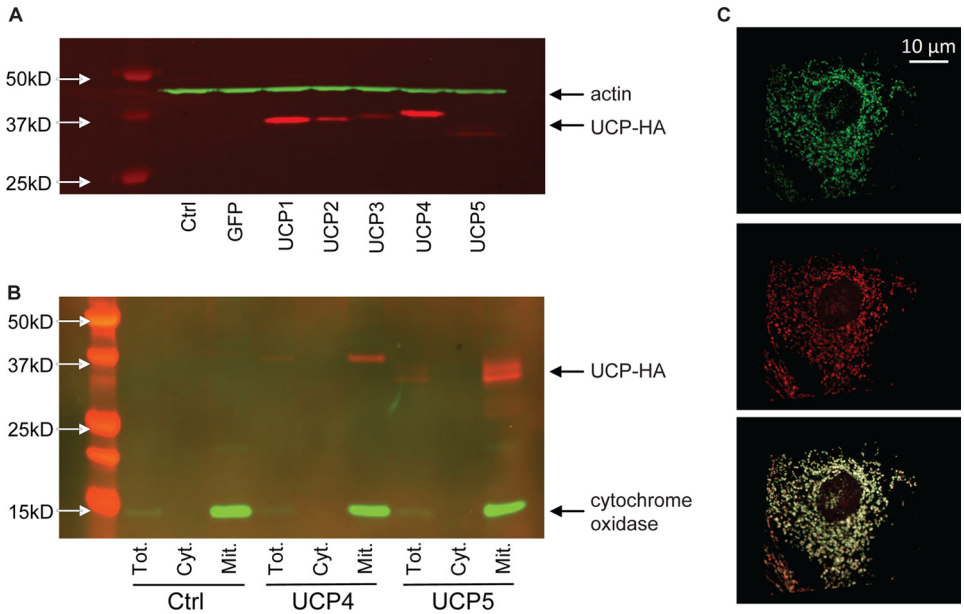

FIGURE 1. **Mitochondrial localization of overexpressed UCPs in astrocytes.** *A*, Western blot showing the expression of each HA-tagged isoform of UCPs. *B*, localization of overexpressed UCP. HA-tagged overexpressed UCP4 and UCP5 were present in the total fraction and were purified in the mitochondrial fraction. *C*, immunohistochemistry showing the co-localization of UCP4-HA (*green*) and cytochrome oxidase (*red*). Thresholded Manders's coefficient (*green versus red channel*) was 0.93, indicating a very high degree of correlation. *Ctrl*, control; *Cyt.*, cytosolic fraction; *Mito.*, mitochondrial fraction; *Tot.*, total fraction.

(control, 99.7 ± 7.4; UCP4over, 92.9 ± 7.6; UCP5over, 92.2 ± 9.3, expressed as percentage of viable cells; n = five independent cells cultured in quadruplicate); there were no statistically significant differences between group means. We also found that UCP overexpression or UCP silencing did not significantly change the mitochondrial mass using a Mitotracker probe not sensitive to the redox state of the mitochondria (control, 99.2 ± 0.2; UCP4over expression, 107.3 ± 2.8; UCP5over expression, 117.2 ± 12.0; UCP4 silencing, 95.6 ± 3.6; UCP5 silencing, 93.5 ± 4.1; expressed as percentages of control; (n = seven independent cells cultures in quadruplicate); there were no statistically significant differences between group means. To assess the UCP4 and UCP5 reduction in astrocytes infected with either the shUCP4 or shUCP5 virus (Fig. 2*C*), we quantified the mRNA level of both UCPs isoforms. We measured a 66% reduction of UCP4 mRNA in astrocytes expressing the shUCP4 and a 94% reduction of UCP5 mRNA in astrocytes expressing the shUCP5. Importantly, the shRNA treatment had an effect only on the targeted UCP expression and not on the expression of the other UCP isoforms.

Effect of Uncoupling Proteins on Astrocytic Glucose Metabolism—As previously described, glutamate released in the synaptic cleft is rapidly cleared by an active uptake into astrocytes. One glutamate is co-transported with three Na^+. Intracellular Na^+ homeostasis is re-established by the Na^+/K^+-ATPase, which requires ATP provided mainly by glycolysis. The resulting lactate is released by astrocytes in extracellular space and contributes to the energetic balance of activated neurons in a mechanism known as the astrocyte-neuron lactate shuttle (35, 36). Because mitochondria play a key role in energy metabolism, we investigated the consequences of modifying UCP expression in astrocytes on the metabolic coupling between astrocytes and neurons. Glucose uptake, lactate release, and glycogen content were measured as an index of astrocytic glucose metabolism. Glutamate promotes glucose uptake into astrocytes (21). Overexpression of different UCP isoforms did not affect glucose uptake either under basal conditions or following glutamate stimulation (Fig. 2*A*) as revealed by the [^{3}H]2-deoxyglucose experiments. Similarly, UCP4 or UCP5 silencing was without effect on basal glucose uptake. However, UCP4 silencing significantly reduced glutamate-stimulated glucose uptake by 34 ± 5.4% compared with control astrocytes (Fig. 2*A*, *arrow*).

It has been shown that during neuronal activation, glutamate exposure increased lactate release from astrocytes (21). Lactate release was measured at the end of the 20-min glucose uptake experiments in control and UCPs overexpressing astrocytes stimulated or not with glutamate. Overexpression of uncoupling proteins did not modify the basal or glutamate-stimulated astrocytic lactate release. In contrast, overexpression of UCP4 or 5 reduced the glycogen content of astrocytes (Fig. 2*B*), suggesting that astrocytes with artificially modified metabolism can metabolically adapt drawing on their glycogen stocks.

UCP4 and UCP5 Reduced the Mitochondrial Function in Astrocytes—The uncoupling proteins derive their name from the uncoupling activity of UCP1 in brown adipose tissue cells. UCP1 dissipates their proton gradient by translocating H^+ across the mitochondrial membrane, thereby producing heat instead of ATP. There is no clear evidence that other UCPs decrease the mitochondrial proton gradient. We have tested the hypothetical uncoupling activity of UCP2, UCP4, and UCP5 in astrocytes by measuring the mitochondrial membrane potential and the ATP/ADP ratio. We observed that the mitochondrial potential is reduced in the presence of overexpressed UCP4 or UCP5 (Fig. 3*A*, *black columns*), but not when UCP2 is overexpressed. Astrocytic UCP4 reduced mitochondrial potential by 6% compared with control and UCP5 reduced the mitochondrial potential of astrocytes by 13%. Surprisingly, UCP1

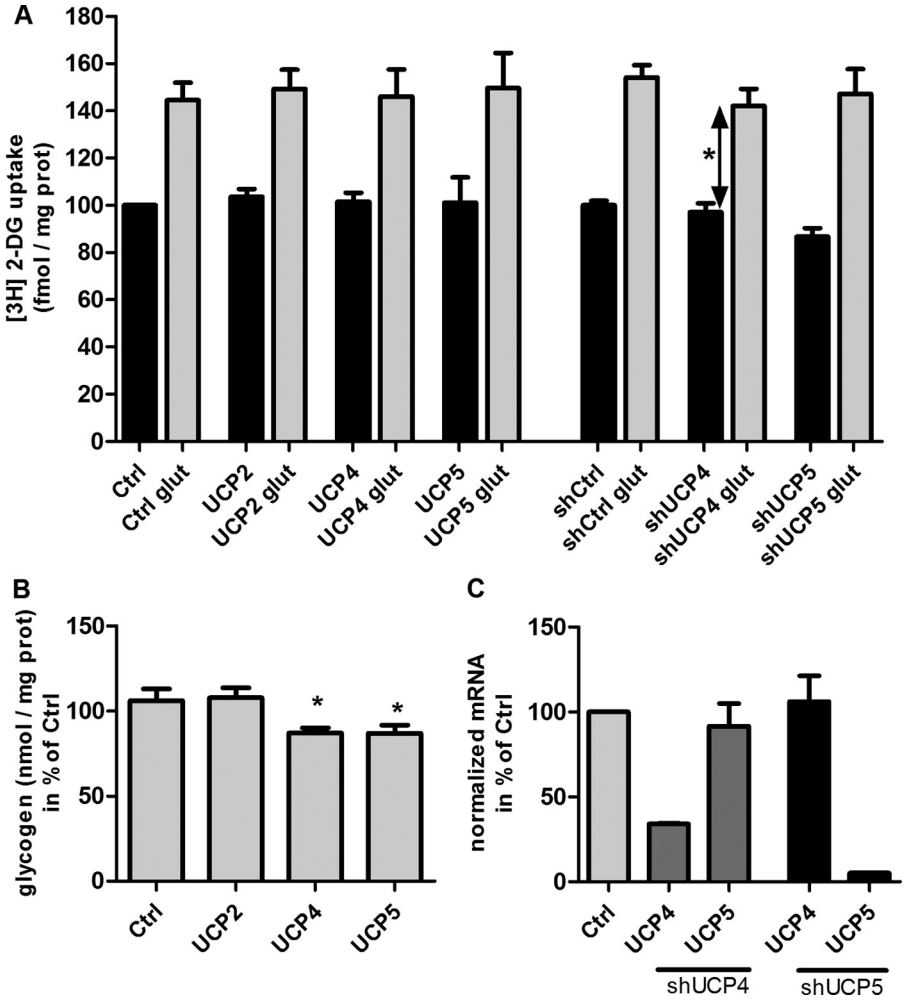

FIGURE 2. **Effects of UCP2, UCP4, and UCP5 on astrocytic glucose metabolism and the effect of silencing with shUCP4,5 on respective mRNA levels.** *A*, glucose uptake before (*black bars*) and after (*gray bars*) glutamate exposure. The presence of glutamate increased glucose uptake by 45%. UCPs overexpression had no effect on glutamate-stimulated glucose uptake. The results are means of triplicates of eight independent experiments. Silencing of UCP4 reduced glutamate-stimulated glucose uptake compared with control conditions. We have subtracted from each value represented by an histogram the value of passive glucose uptake obtained when glucose transporter are blocked with cytochalasin B. *B*, overexpression of UCP4 and UCP5 reduced glycogen content compared with control conditions. The results are means of triplicates of six independent experiments. *C*, mRNA level of UCP4 and UCP5 genes in astrocytes expressing either the shUCP4 or shUCP5. *Ctrl*, control; *2-DG*, 2-deoxyglucose; *glut*, glutamate.

overexpression had no effect on the mitochondrial potential of astrocytes (not shown). This suggests that UCP activity is tissue-specific. Silencing of UCP4 and UCP5 had the opposite effect to overexpression, resulting in an increase in the mitochondrial potential by 10% (Fig. 3*A*, *gray columns*). These results confirm the implication of UCP4 and UCP5 in mitochondrial potential in astrocytes.

In mitochondria, ATP production is closely linked to the proton gradient across the inner mitochondrial membrane. Because ATP synthase requires the proton motive force to produce ATP, it is expected that a reduction in mitochondrial potential leads to a reduction in ATP formation. Accordingly, overexpression of UCP4 or UCP5 significantly decreases the ATP/ADP ratio in astrocytes by 12–14% (Fig. 3*B*, *black columns*). These results suggested a leak of protons from the intramitochondrial matrix via uncoupling proteins, which led to a decreased activity of the FoF1-ATP synthase. Silencing yielded the reverse effect for both UCP4 and 5, *i.e.* increased the ATP/ADP ratio by 20%, supporting this conclusion (Fig. 3*B*, *gray columns*).

A possible role for the uncoupling protein described in the literature (for review, see Ref. 37) is the reduction of ROS production. Indeed, a mild uncoupling has been shown to have a moderating effect on oxidative stress. We tested this protective effect for the two brain isoforms of uncoupling proteins in astrocytes. We chose to measure superoxide anion production as an index of ROS production. However, because of its very short half-life, we quantified H_2O_2 release as an alternative. Overexpression of UCP4 or UCP5 significantly reduced H_2O_2 release into the medium of astrocyte cultures by 9–11% compared with control cells (Fig. 3*C*, *black columns*). In contrast, silencing of UCP4 and UCP5 resulted in enhanced H_2O_2 release by 127 and 133%, respectively, of control cells (Fig. 3*C*, *gray columns*).

UCP4 Enhanced TCA Cycle Activity in Astrocytes—The TCA cycle plays a key role in energy production: its activity can be monitored by determining the NAD^+/NADH ratio and CO_2 production. The NAD^+/NADH ratio is an important component of the *redox state* of a cell; it is controlled by the activity of several enzymes, including glyceraldehyde-3-phosphate dehy-

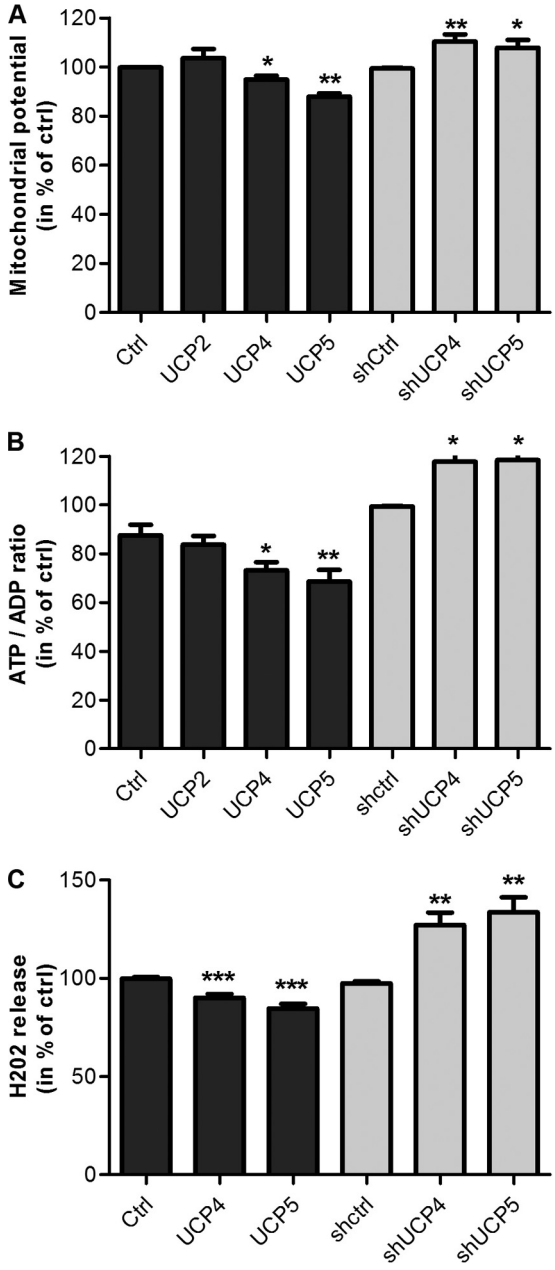

FIGURE 3. **UCP4 and UCP5 reduced the mitochondrial function in astrocytes.** *A*, mitochondrial electrical potential was reduced in the presence of overexpressed UCP4 and UCP5 (*black bars*). Overexpression of UCP2 did not modify the electrical potential of astrocytes. Control astrocytes are infected with a virus containing the GFP sequence. The silencing of these two isoforms increased the mitochondrial potential (*gray bars*), and control astrocytes are infected with a virus targeting the GFP sequence. The results are means of quadruplicates of at least 12 independent experiments. *B*, the ATP/ADP ratio was reduced in the presence of overexpressed UCP4 and UCP5 (*black bars*); opposite effects were obtained with the silencing (*gray bars*). Overexpression of UCP2 did not modify the ATP/ADP ratio of astrocytes. The results are means of quadruplicate of at least 12 independent experiments. *C*, UCP4 and UCP5 overexpression (*black bars*) reduced H_2O_2 level found in medium, whereas silencing of UCP4 or UCP5 (*gray bars*) increased the release of H_2O_2. The results are means of quadruplicates of at least 14 independent experiments. *Ctrl*, control.

drogenase and pyruvate dehydrogenase. The TCA cycle is an important source of NADH providing reducing equivalents to the respiratory chain. Astrocytes overexpressing UCP4 showed a 33% reduction of the NAD^+/NADH ratio compared with control astrocytes (Fig. 4*A*, *black columns*). In contrast, UCP4 silencing increased the ratio by 148% of control levels (Fig. 4*A*, *gray columns*), suggesting that the cell is in a more reduced state in these conditions. Modulation of UCP5 expression was without effect.

The decrease in the NAD^+/NADH ratio observed following UCP4 overexpression could result both from an increase in the TCA cycle activity and/or a reduced activity of the respiratory chain. Because we found that oxidative phosphorylation was decreased (mitochondrial potential and ATP/ADP ratio) following UCP4 overexpression, we wanted to investigate whether the TCA cycle activity was reduced as well. To test this hypothesis, we measured the CO_2 production from glucose radioactively labeled in C1 or C6 to differentiate CO_2 production caused by the TCA cycle from total CO_2 produced. We observed that CO_2 production by the TCA cycle was increased by 31% in the presence of overexpressed UCP4 (Fig. 4*B*). Overexpression of UCP5 had no significant effect.

Effects of UCP4 and UCP5 on Mitochondrial Respiration in Astrocytes and Relation to Mitochondrial Acidification—Having determined that UCP4 and UCP5 had an uncoupling activity by modifying the mitochondrial potential, the ATP/ADP ratio, the H_2O_2 level, and NAD/NADH ratio and that UCP4 also affected the TCA cycle, we set out to determine the role of UCPs in the final element of the electron transport chain, namely the oxygen consumption. We analyzed the effect of overexpressed or silenced UCP4 and UCP5 in astrocytes on the OCR. We measured the respiration profile of astrocytes for 2 h including application of various compounds. We compared the OCR of control astrocytes and astrocytes overexpressing or silenced for UCP4 after 200 μM glutamate stimulation (Fig. 5*A*). We had previously shown that glutamate reduced the OCR in astrocytes, a phenomenon dependent on the mitochondrial matrix acidification (20). We could thus assume that if the mitochondrial matrix acidification and the mitochondrial potential reduction were linked and somehow controlled via an UCP, we could expect that the astrocytic OCR decrease in the presence of glutamate would be enhanced when overexpressing uncoupling proteins. We therefore measured the basal and glutamate-stimulated OCR in astrocytes overexpressing or silenced for UCP4 and UCP5. Glutamate application on astrocyte reduced OCR by 11% compared with basal level (Fig. 5*A*). The OCR represented in Fig. 5*B* are showing that in nomal medium astrocyte overexpressing UCP4 do have and higher OCR, because the ATP/ADP ratio is reduced and mitochondrial potential is reduced. The silencing of UCP4 in these conditions also shows a higher OCR than in control condition, because we made these respiration measurements in the presence of deoxy-glucose, which blocks glycolysis. Abundance or reduction of UCP4 in astrocyte modified the OCR response to glutamate (Fig. 5*C*). Indeed, in the presence of glutamate, overexpression of UCP4 decreased OCR by 16%; conversely, silencing of UCP4 decreased the OCR by only 2%.

As previously mentioned, the effects of glutamate on oxygen consumption rate were shown to depend on the mitochondrial matrix acidification (20). We tested the implication of uncoupling proteins on this acidification by measuring the mitochondrial pH in astrocytes overexpressing UCP4 or UCP5, before

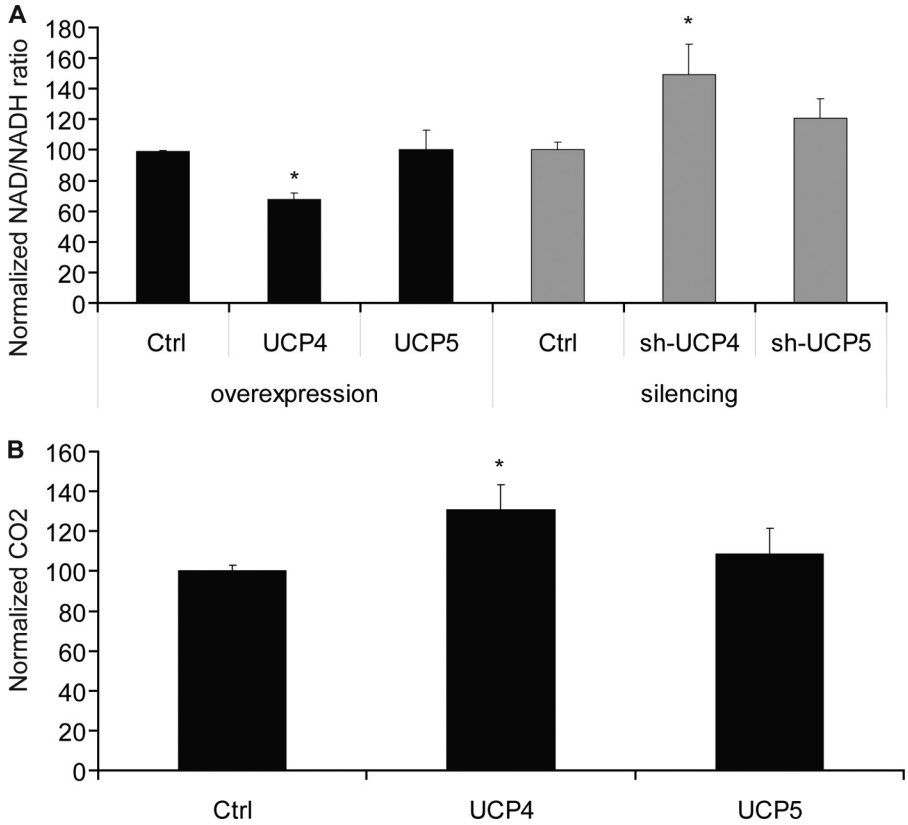

FIGURE 4. **UCP4 enhanced the glycolytic activity of astrocyte.** *A*, the NAD^+/NADH ratio was reduced in the presence of overexpressed UCP4 and increased by UCP4 silencing. UCP5 had no significant effect on NAD^+/NADH. The results are means of triplicates of at least seven independent experiments. *B*, UCP4 overexpression increased CO_2 production from the TCA cycle. No significant effects were found for UCP5 overexpression. The results are means of triplicates of six independent experiments. *Ctrl*, control.

and after stimulation by 200 μM glutamate. Overexpression of UCP4 reduced significantly the basal mitochondrial matrix pH from pH 7.31 ± 0.06 in control cells to pH 7.05 ± 0.08 in infected cells (Fig. 6). UCP4 silencing did not significantly affect basal mitochondrial matrix pH, nor did UCP5 overexpression or silencing. In control cells, glutamate application decreased mitochondrial matrix to pH 6.64 ± 0.1, whereas UCP4 silencing decreased pH to 6.88 ± 0.05, therefore causing a milder acidification. UCP5 did not significantly modify the basal or the glutamate-stimulated matrix pH neither in overexpression nor in silencing. These results indicate that UCP4 is involved in the glutamate-induced mitochondrial matrix acidification, which is the likely cause of its effect on mitochondrial respiration.

UCP4-mediated Lactate Release from Astrocytes Improve Neuronal Survival—It has already been demonstrated that astrocyte-derived lactate is an important energy substrate for neurons (12, 38–41). As an index of metabolic activity in neurons, we measured the OCR of neurons exposed to the two most relevant energy substrates, namely glucose and lactate. As reported in Fig. 7*A*, the OCR is markedly increased in neurons exposed to lactate (50 mM) alone compared with a mix of glucose (12.5 mM) and lactate (25 mM) or to glucose alone (25 mM). All substrates or mixtures thereof were tested at equicaloric final concentrations. Given the role of astrocytes in providing lactate to neurons, we set out to study the possible involvement of astrocytic uncoupling protein level of expression on lactate production and in neuronal survival.

The release of lactate, accumulated for 24 h, was increased by 16% in astrocytes overexpressing UCP4 compared with control astrocytes (Fig. 7*B*, *black columns*). UCP5 overexpression had no significant effect on lactate release. Silencing of UCP4 or UCP5 reduced lactate release to 88 ± 4.2 and 80 ± 2.6% of control values, respectively (Fig. 7*B*, *gray columns*).

Because neurons exposed to lactate increased their respiratory rate (Fig. 7*A*), we measured the viability of neurons co-cultured with astrocytes overexpressing or silenced for UCP4/UCP5. Overexpression of UCP4 or UCP5 in astrocytes increased the neuronal survival by nearly 20–35% compared with control astrocytes (Fig. 7*C*, *black columns*). In contrast, UCP4 or UCP5 silencing in astrocytes reduced significantly the viability of co-cultured neurons by 33 and 24%, respectively (Fig. 7*C*, *gray columns*).

DISCUSSION

The decoupling of proton gradient dedicated to the production of ATP in favor of a decrease in entropy and hence an increase in temperature is a well described (1, 42, 43) phenomenon in brown adipose tissue and is caused by the presence of UCP1 in this tissue. In brain cells, UCP1 is marginally expressed, and its possible role in the CNS remains unclear.

The UCP2 isoform role in the brain is still debated, but it appears to be linked either to controlling the local temperature to increase conduction velocity (4) or to controlling ROS production (5). Regarding this control of ROS by UCP2, this role

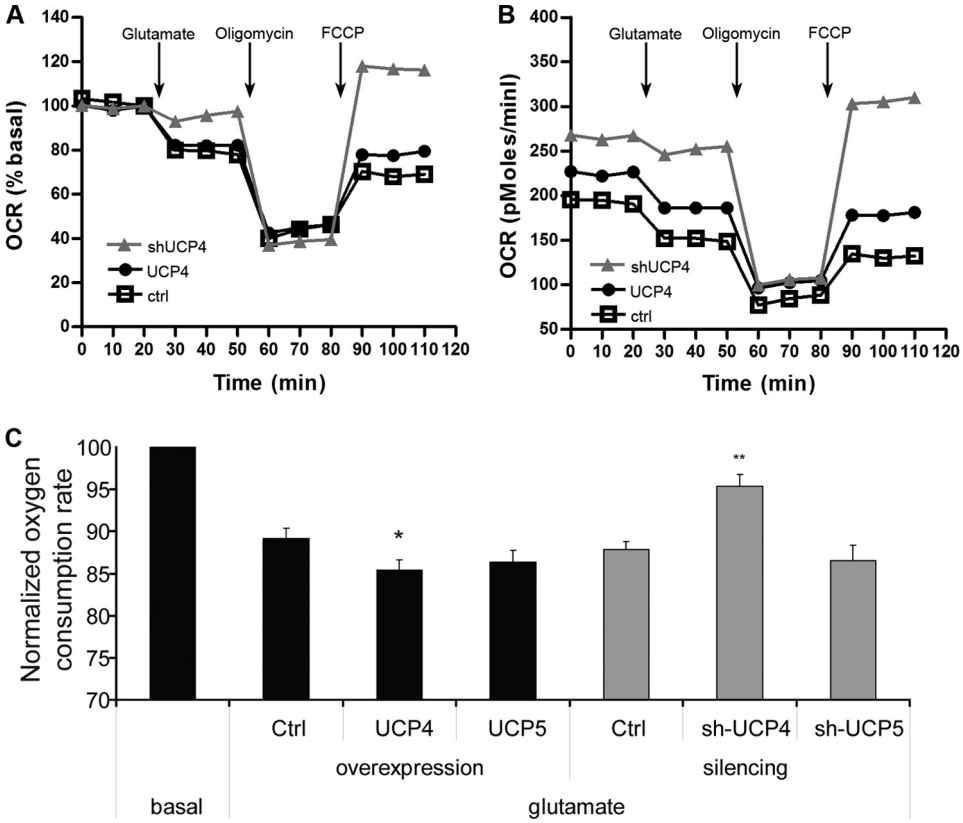

FIGURE 5. **Effects of UCP4 and UCP5 on mitochondrial respiration in astrocytes.** *A*, time course of OCR, as a percentage of basal respiration calculated from the third time points, in the presence of overexpressed or silenced UCP4. UCP4 increased the effect of glutamate, whereas UCP4 silencing reduced it, suggesting an UCP4-depending mechanism of glutamate on OCR. The results are means of quintuplicates of one representative experiment. *B*, time course of OCR without normalization. *C*, quantification of oxygen consumption rate. Under glutamate exposure, UCP4 overexpression reduced the OCR compared with control astrocytes. In the same vein, the OCR under glutamate was higher in astrocytes silenced for UCP4 compared with control astrocytes. No significant results were found for UCP5. The results are means of septuplicates of six independent experiments. *Ctrl*, control; *FCCP*, carbonyl cyanide-4-(trifluoromethoxy)phenylhydrazone.

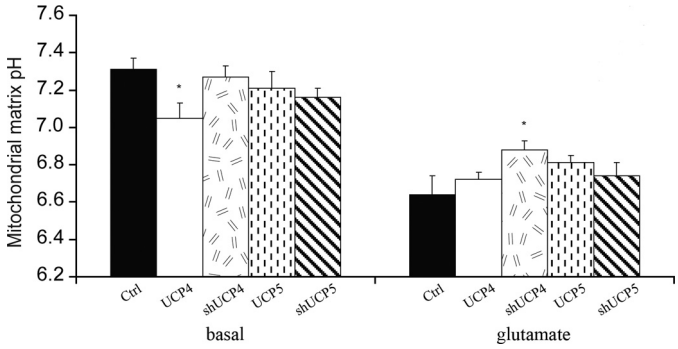

FIGURE 6. **UCP4 is required for the mitochondrial matrix acidification following glutamate exposure.** Glutamate exposure induced a mitochondrial matrix acidification. UCP4 overexpression reduced the basal matrix pH, whereas UCP4 silencing reduced the acidification caused by glutamate stimulation, suggesting that the matrix acidification following glutamate exposure is an UCP4-dependent mechanism. UCP5 had no significant effects. The results are means of at least 10 experiments. *Ctrl*, control.

seems to be measured not only in the CNS, but in most studied tissues. UCP3 isoform appears to be expressed exclusively in muscle and is found certainly in a nonspecific manner in the brain. Our overexpression of the five isoforms with an HA tag in astrocytes in culture was used to validate the method of expression of the protein and also allowed confirmation that none of the commercial antibodies directed against one or the other UCPs isoforms was really specific.

The primary aim of this study was to elucidate the role of UCP4 and UCP5 isoforms in the CNS. Localization of UCP4 and UCP5 in the mouse brain (16, 19) demonstrates an important RNA expression that is likely to be translated into a functional role. Brain cell metabolism is tightly regulated, and its perturbation can lead to dysfunction and maybe to neurodegenerative diseases as discussed by Andrews *et al.* (44). It therefore becomes important to understand UCP4 and UCP5 functions, mechanisms of action, and, in particular, their involvement in metabolism in astrocytes, given the intimate metabolic relationship between astrocytes and neurons.

We first confirmed the earlier observation (21) that glutamate leads to a stimulation of glucose uptake by 20% and found that the same happens in astrocytes overexpressing UCP4 or UCP5. However, when endogenous UCP4 was reduced using sh-UCP4 (Fig. 2*A*), this enhancement of glucose uptake caused by glutamate did not occur. This observation was parallel to lactate release, which was similarly influenced by UCP4. Thus, we hypothesized that UCP4 operates a control on respiration (Fig. 5*A*) by tuning intramitochondrial pH level as we observed (20) in the presence of glutamate.

The reduced level of glycogen in astrocytes overexpressing UCP4 or UCP5 may be a consequence of the mitochondrial uncoupling observed and hence to the reduction of the available ATP in cell. One ATP is necessary to transform glucose to glucose 1-phosphate, which is the first step in the glycogen synthesis.

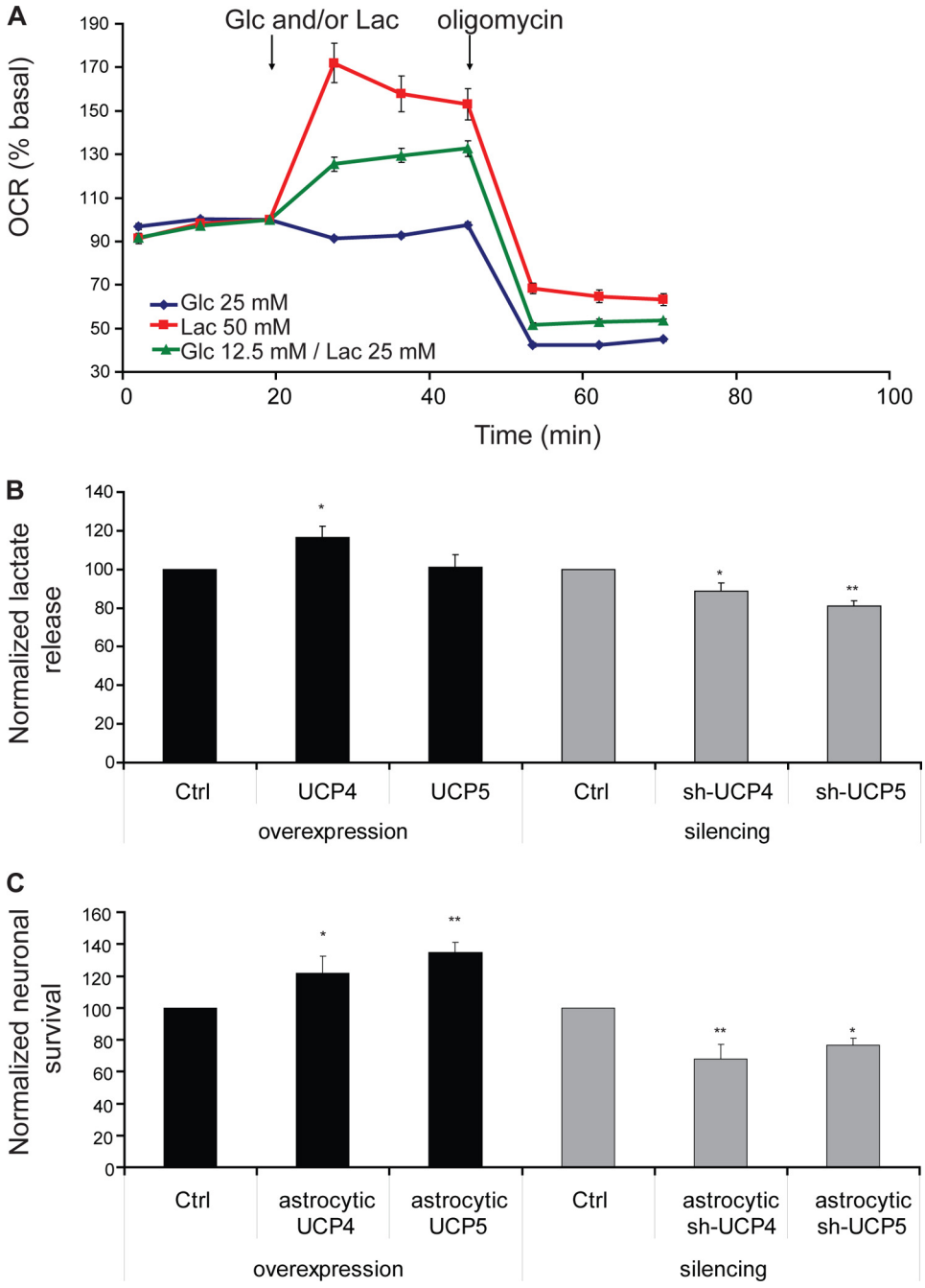

FIGURE 7. **Astrocytic UCP4-mediated lactate release increased neuronal survival.** *A*, time course of OCR in neurons depending on substrate availability. Neurons preincubated with 0.5 mM glucose increased their OCR when they received glucose + lactate, but the higher OCR was obtained with high concentration of lactate alone. The results presented are means of quintuplicates. *B*, 24 h lactate released by astrocytes overexpressing or silenced for UCP4 or UCP5. UCP4 overexpression increased lactate release, whereas UCP5 overexpression had no significant effects. On the other hand, lactate released by astrocytes was reduced when UCP4 or UCP5 were silenced. The results are means of triplicates of 10 experiments. *C*, neurons exposed to astrocytes overexpressing UCP4 or UCP5 showed an increased viability compared with neurons exposed to control astrocytes. On the other hand, neurons exposed to astrocytes silenced for UCP4 or UCP5 had a reduced viability compared with neurons exposed to control astrocytes. The results are means of triplicates of nine experiments. *Ctrl*, control; *Glc*, glucose; *Lac*, lactate.

At the astrocyte mitochondrial level, the effects observed during the overexpression of UCP4 or 5 are decreased mitochondrial electrical potential, decreased ATP production, and decreased H_2O_2 production (Fig. 8). One can deduce from these results that overexpression of UCP4 or 5 decreases the efficiency of oxidative phosphorylation. Under these conditions, the Krebs cycle is enhanced, which results in a decrease of the NAD/NADH ratio, and also by an increase in the CO_2 production. This increase in NADH and CO_2 from the Krebs cycle is possible because there is no exhaustion of the substrates (ADP, NAD, and acetyl-CoA) and no negative regulation by ATP. It also indicates that the production of reducing equivalents (NADH) has not reached the threshold of inhibition as evidenced by the accumulation of CO_2 coming from the Krebs cycle that keeps functioning.

All mitochondrial indices tested (ATP production, H_2O_2 production, mitochondrial potential, and NAD/NADH ratio) were confirmed by the opposite effects elicited by UCP4 or UCP5

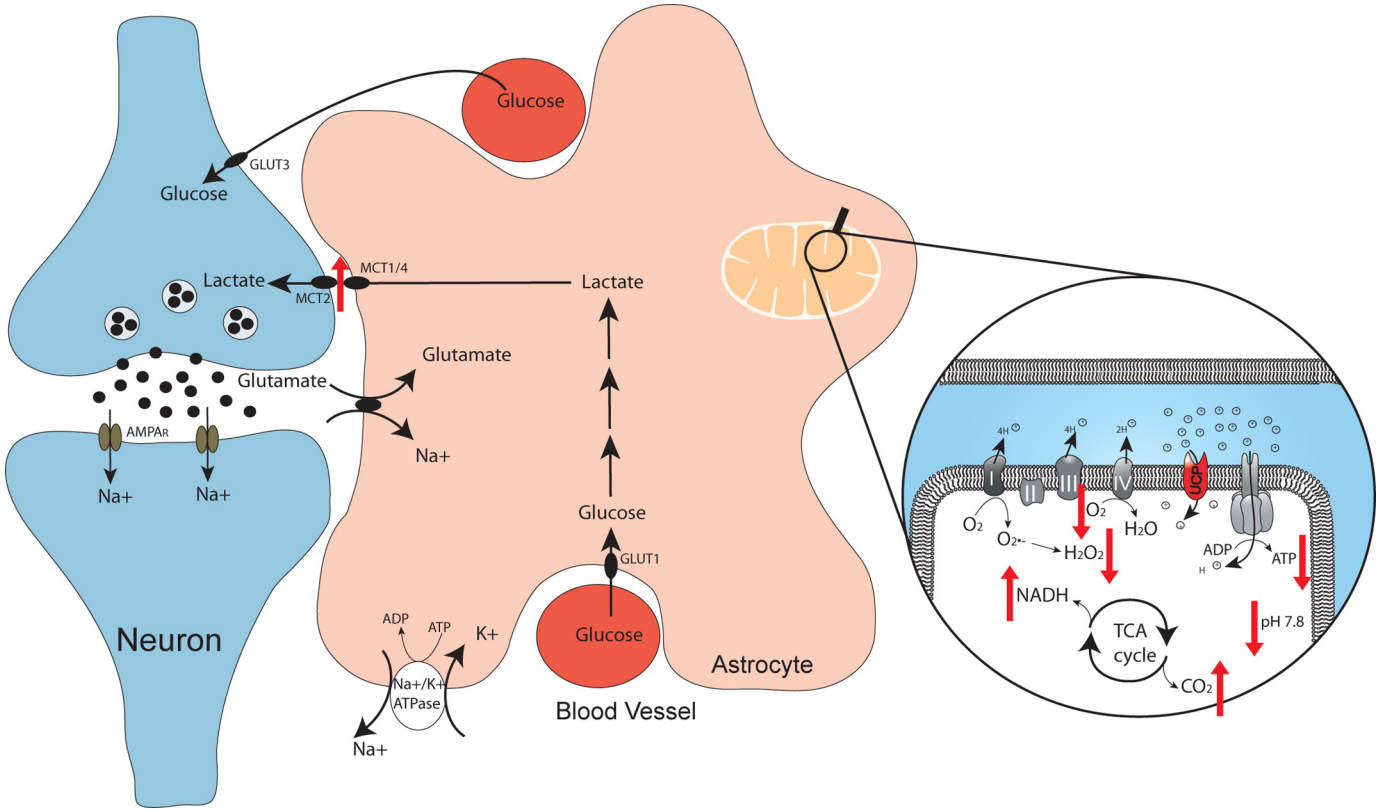

FIGURE 8. **Effect of astrocytic uncoupling protein on astrocyte-neuron lactate shuttle hypothesis.** When UCP4 was overexpressed in astrocytes, some metabolic changes occurred on the cell as shown by *red arrows*. Uncoupling activity was detected by reduced mitochondrial potential and reduced ATP/ADP ratio. TCA cycle activity was enhanced as shown by increased NADH (decreased NAD^+/NADH ratio) and increased CO_2 production. Astrocytes overexpressing UCP4 had reduced H_2O_2 production, decreased oxygen consumption rate, and increased lactate release. In the presence of astrocytes overexpressing UCP4, neighboring neurons survived better.

silencing, demonstrating the essential role of UCPs in astrocytes in the mitochondrial respiration control. According to the results presented in this study, the mode of action of UCP4 on mitochondria in astrocytes can be summarized in an uncoupling of oxidative phosphorylation. It is likely that the same applies to UCP5, also expressed by astrocyte mitochondria.

The next issue is to identify a functional role for these UCPs. We have previously shown (20) that astrocytes OCR decreased by 20% following glutamate application and that this decrease in respiration was due to mitochondrial acidification. We now show that the decrease in pH is controlled by UCP4. Overexpression of UCP4 actually decreased basal intramitochondrial pH, and glutamate application caused an additional acidification to reach the same pH 6.6 as in the nontransfected astrocytes. This pH value likely represents the lower limit of matrix acidification. This decrease in pH in all cases had the same effect of reducing the respiration by 20%. The demonstration of the role played by UCP4 in controlling respiration via the intramitochondrial pH is even more striking when we reduced the UCP4 expression. In this case, the intramitochondrial pH drop was less pronounced in the presence of glutamate, and respiration is consequently not decreased to the same extent.

The results of the UCP5 experiments do not allow clear-cut conclusions regarding its mode of action. It is noteworthy that UCP5 can be found in two different variants (9). For this study, we cloned the full-length sequence in astrocyte; it is conceivable that the UCP5 short variant is the form present in astrocytes, whereas the long form is present in neurons, or the other way round. Further investigations need to be undertaken to clarify by which mechanism astrocyte UCP5 increases neuronal viability.

UCP4 function would then be that of reducing astrocyte respiration in the presence of glutamate, through a decrease in intramitochondrial pH. To compensate for the impaired oxidative energy production, astrocytes enhance glycolysis, and therefore their production of lactate. Lactate produced by astrocytes is used by neurons, as demonstrated by the OCR increase caused by lactate in neuronal cultures and has the beneficial effect of enhancing their survival rate, as shown in Fig. 7*C*.

CONCLUSION

In summary, the release of glutamate in synapses and reuptake by astrocytes induces a mechanism of decreased respiration in astrocyte, an effect mediated by UCP4, and possibly UCP5, whose consequence is to promote energy production by glycolysis for producing preferentially lactate that can be in turn used by neurons (Fig. 8). Overall, control of pH by the intramitochondrial UCP4 in astrocytes may be considered as a mechanism that helps sustain neuronal survival. Therefore, it is not surprising that a modification in UCP4 expression was found at the onset of neurodegenerative diseases (11, 45, 46). This work explains for the first time a role for the presence of UCP4 in the brain.

Acknowledgments—We thank the members of the Bioimaging and Optics Platform (Ecole Polytechnique Fédérale de Lausanne, Lausanne, Switzerland) for sharing expertise in image acquisition and statistical analysis.

REFERENCES

1. Nicholls, D. G., Bernson, V. S., and Heaton, G. M. (1978) The identification of the component in the inner membrane of brown adipose tissue mitochondria responsible for regulating energy dissipation. *Experientia Suppl.* **32,** 89–93
2. Kozak, L. P., Britton, J. H., Kozak, U. C., and Wells, J. M. (1988) The mitochondrial uncoupling protein gene. Correlation of exon structure to transmembrane domains. *J. Biol. Chem.* **263,** 12274–12277
3. Bouillaud, F., Raimbault, S., and Ricquier, D. (1988) The gene for rat uncoupling protein: complete sequence, structure of primary transcript and evolutionary relationship between exons. *Biochem. Biophys. Res. Commun.* **157,** 783–792
4. Horvath, T. L., Warden, C. H., Hajos, M., Lombardi, A., Goglia, F., and Diano, S. (1999) Brain uncoupling protein 2: uncoupled neuronal mitochondria predict thermal synapses in homeostatic centers. *J. Neurosci.* **19,** 10417–10427
5. Arsenijevic, D., Onuma, H., Pecqueur, C., Raimbault, S., Manning, B. S., Miroux, B., Couplan, E., Alves-Guerra, M. C., Goubern, M., Surwit, R., Bouillaud, F., Richard, D., Collins, S., and Ricquier, D. (2000) Disruption of the uncoupling protein-2 gene in mice reveals a role in immunity and reactive oxygen species production. *Nat. Genet.* **26,** 435–439
6. Boss, O., Bobbioni-Harsch, E., Assimacopoulos-Jeannet, F., Muzzin, P., Munger, R., Giacobino, J. P., and Golay, A. (1998) Uncoupling protein-3 expression in skeletal muscle and free fatty acids in obesity. *Lancet* **351,** 1933
7. Boss, O., Samec, S., Kühne, F., Bijlenga, P., Assimacopoulos-Jeannet, F., Seydoux, J., Giacobino, J. P., and Muzzin, P. (1998) Uncoupling protein-3 expression in rodent skeletal muscle is modulated by food intake but not by changes in environmental temperature. *J. Biol. Chem.* **273,** 5–8
8. Alán, L., Smolková, K., Kronusová, E., Santorová, J., and Jezek, P. (2009) Absolute levels of transcripts for mitochondrial uncoupling proteins UCP2, UCP3, UCP4, and UCP5 show different patterns in rat and mice tissues. *J. Bioenerg. Biomembr.* **41,** 71–78
9. Yu, X. X., Mao, W., Zhong, A., Schow, P., Brush, J., Sherwood, S. W., Adams, S. H., and Pan, G. (2000) Characterization of novel UCP5/BMCP1 isoforms and differential regulation of UCP4 and UCP5 expression through dietary or temperature manipulation. *FASEB J.* **14,** 1611–1618
10. Liu, D., Chan, S. L., de Souza-Pinto, N. C., Slevin, J. R., Wersto, R. P., Zhan, M., Mustafa, K., de Cabo, R., and Mattson, M. P. (2006) Mitochondrial UCP4 mediates an adaptive shift in energy metabolism and increases the resistance of neurons to metabolic and oxidative stress. *Neuromolecular Med.* **8,** 389–414
11. Wu, Z., Zhang, J., and Zhao, B. (2009) Superoxide anion regulates the mitochondrial free Ca2+ through uncoupling proteins. *Antioxid. Redox Signal.* **11,** 1805–1818
12. Bélanger, M., Allaman, I., and Magistretti, P. J. (2011) Brain energy metabolism: focus on astrocyte-neuron metabolic cooperation. *Cell Metab.* **14,** 724–738
13. Sanchis, D., Fleury, C., Chomiki, N., Goubern, M., Huang, Q., Neverova, M., Grégoire, F., Easlick, J., Raimbault, S., Lévi-Meyrueis, C., Miroux, B., Collins, S., Seldin, M., Richard, D., Warden, C., Bouillaud, F., and Ricquier, D. (1998) BMCP1, a novel mitochondrial carrier with high expression in the central nervous system of humans and rodents, and respiration uncoupling activity in recombinant yeast. *J. Biol. Chem.* **273,** 34611–34615
14. Mao, W., Yu, X. X., Zhong, A., Li, W., Brush, J., Sherwood, S. W., Adams, S. H., and Pan, G. (1999) UCP4, a novel brain-specific mitochondrial protein that reduces membrane potential in mammalian cells. *FEBS Lett.* **443,** 326–330
15. Chan, S. L., Liu, D., Kyriazis, G. A., Bagsiyao, P., Ouyang, X., and Mattson, M. P. (2006) Mitochondrial uncoupling protein-4 regulates calcium homeostasis and sensitivity to store depletion-induced apoptosis in neural cells. *J. Biol. Chem.* **281,** 37391–37403
16. Smorodchenko, A., Rupprecht, A., Sarilova, I., Ninnemann, O., Bräuer, A. U., Franke, K., Schumacher, S., Techritz, S., Nitsch, R., Schuelke, M., and Pohl, E. E. (2009) Comparative analysis of uncoupling protein 4 distribution in various tissues under physiological conditions and during development. *Biochim. Biophys. Acta* **1788,** 2309–2319
17. Kim-Han, J. S., Reichert, S. A., Quick, K. L., and Dugan, L. L. (2001) BMCP1: a mitochondrial uncoupling protein in neurons which regulates mitochondrial function and oxidant production. *J. Neurochem.* **79,** 658–668
18. Pichiule, P., Chavez, J. C., and LaManna, J. C. (2003) Oxygen and oxidative stress modulate the expression of uncoupling protein-5 in vitro and in vivo. *Adv. Exp. Med. Biol.* **540,** 103–107
19. Huang, P. S., Son, J. H., Abbott, L. C., and Winzer-Serhan, U. H. (2011) Regulated expression of neuronal SIRT1 and related genes by aging and neuronal β2-containing nicotinic cholinergic receptors. *Neuroscience* **196,** 189–202
20. Azarias, G., Perreten, H., Lengacher, S., Poburko, D., Demaurex, N., Magistretti, P. J., and Chatton, J. Y. (2011) Glutamate transport decreases mitochondrial pH and modulates oxidative metabolism in astrocytes. *J. Neurosci.* **31,** 3550–3559
21. Pellerin, L., and Magistretti, P. J. (1994) Glutamate uptake into astrocytes stimulates aerobic glycolysis: a mechanism coupling neuronal activity to glucose utilization. *Proc. Natl. Acad. Sci. U.S.A.* **91,** 10625–10629
22. Sorg, O., and Magistretti, P. J. (1992) Vasoactive intestinal peptide and noradrenaline exert long-term control on glycogen levels in astrocytes: blockade by protein synthesis inhibition. *J. Neurosci.* **12,** 4923–4931
23. Allaman, I., Pellerin, L., and Magistretti, P. J. (2004) Glucocorticoids modulate neurotransmitter-induced glycogen metabolism in cultured cortical astrocytes. *J. Neurochem.* **88,** 900–908
24. Smiley, S. T., Reers, M., Mottola-Hartshorn, C., Lin, M., Chen, A., Smith, T. W., Steele, G. D., Jr., and Chen, L. B. (1991) Intracellular heterogeneity in mitochondrial membrane potentials revealed by a J-aggregate-forming lipophilic cation JC-1. *Proc. Natl. Acad. Sci. U.S.A.* **88,** 3671–3675
25. Reers, M., Smith, T. W., and Chen, L. B. (1991) J-aggregate formation of a carbocyanine as a quantitative fluorescent indicator of membrane potential. *Biochemistry* **30,** 4480–4486
26. Zhou, M., Diwu, Z., Panchuk-Voloshina, N., and Haugland, R. P. (1997) A stable nonfluorescent derivative of resorufin for the fluorometric determination of trace hydrogen peroxide: applications in detecting the activity of phagocyte NADPH oxidase and other oxidases. *Anal. Biochem.* **253,** 162–168
27. Haskew-Layton, R. E., Payappilly, J. B., Smirnova, N. A., Ma, T. C., Chan, K. K., Murphy, T. H., Guo, H., Langley, B., Sultana, R., Butterfield, D. A., Santagata, S., Alldred, M. J., Gazaryan, I. G., Bell, G. W., Ginsberg, S. D., and Ratan, R. R. (2010) Controlled enzymatic production of astrocytic hydrogen peroxide protects neurons from oxidative stress via an Nrf2-independent pathway. *Proc. Natl. Acad. Sci. U.S.A.* **107,** 17385–17390
28. Zerez, C. R., Lee, S. J., and Tanaka, K. R. (1987) Spectrophotometric determination of oxidized and reduced pyridine nucleotides in erythrocytes using a single extraction procedure. *Anal. Biochem.* **164,** 367–373
29. Allaman, I., Gavillet, M., Belanger, M., Laroche, T., Viertl, D., Lashuel, H. A., and Magistretti, P. J. (2010) Amyloid-β aggregates cause alterations of astrocytic metabolic phenotype: impact on neuronal viability. *J. Neurosci.* **30,** 3326–3338
30. Demaurex, N., and Poburko, D. (2009) Modulation of mitochondrial proton gradients by the plasma membrane calcium ATPase. *J. Physiol. Sci.* **59,** (Suppl. 1) 348
31. Chatton, J. Y., Marquet, P., and Magistretti, P. J. (2000) A quantitative analysis of L-glutamate-regulated Na^+ dynamics in mouse cortical astrocytes: implications for cellular bioenergetics. *Eur. J. Neurosci.* **12,** 3843–3853
32. Rosenberg, J. C., and Rush, B. F. (1966) An enzymatic-spectrophotometric determination of pyruvic and lactic acid in blood. Methodologic aspects. *Clin. Chem.* **12,** 299–307
33. Mosmann, T. (1983) Rapid colorimetric assay for cellular growth and survival: application to proliferation and cytotoxicity assays. *J. Immunol. Methods* **65,** 55–63

34. Lengacher, S., Magistretti, P. J., and Pellerin, L. (2004) Quantitative rt-PCR analysis of uncoupling protein isoforms in mouse brain cortex: methodological optimization and comparison of expression with brown adipose tissue and skeletal muscle. *J. Cereb. Blood Flow Metab.* **24,** 780–788
35. Bittar, P. G., Charnay, Y., Pellerin, L., Bouras, C., and Magistretti, P. J. (1996) Selective distribution of lactate dehydrogenase isoenzymes in neurons and astrocytes of human brain. *J. Cereb. Blood Flow Metab.* **16,** 1079–1089
36. Pellerin, L., Pellegri, G., Bittar, P. G., Charnay, Y., Bouras, C., Martin, J. L., Stella, N., and Magistretti, P. J. (1998) Evidence supporting the existence of an activity-dependent astrocyte-neuron lactate shuttle. *Dev. Neurosci.* **20,** 291–299
37. Jezek, P., Zácková, M., Růzicka, M., Skobisová, E., and Jabůrek, M. (2004) Mitochondrial uncoupling proteins: facts and fantasies. *Physiol. Res.* **53,** S199–S211
38. Magistretti, P. J., Pellerin, L., Rothman, D. L., and Shulman, R. G. (1999) Energy on demand. *Science* **283,** 496–497
39. Pellerin, L., and Magistretti, P. J. (2004) Neuroscience. Let there be (NADH) light. *Science* **305,** 50–52
40. Lee, Y., Morrison, B. M., Li, Y., Lengacher, S., Farah, M. H., Hoffman, P. N., Liu, Y., Tsingalia, A., Jin, L., Zhang, P. W., Pellerin, L., Magistretti, P. J., and Rothstein, J. D. (2012) Oligodendroglia metabolically support axons and contribute to neurodegeneration. *Nature* **487,** 443–448
41. Suzuki, A., Stern, S. A., Bozdagi, O., Huntley, G. W., Walker, R. H., Magistretti, P. J., and Alberini, C. M. (2011) Astrocyte-neuron lactate transport is required for long-term memory formation. *Cell* **144,** 810–823
42. Nicholls, D. G., and Locke, R. M. (1984) Thermogenic mechanisms in brown fat. *Physiol. Rev.* **64,** 1–64
43. Ricquier, D. (2006) Fundamental mechanisms of thermogenesis. *C. R. Biol.* **329,** 578–586; discussion 653–575
44. Andrews, Z. B., Diano, S., and Horvath, T. L. (2005) Mitochondrial uncoupling proteins in the CNS: in support of function and survival. *Nat. Rev. Neurosci.* **6,** 829–840
45. de la Monte, S. M., and Wands, J. R. (2006) Molecular indices of oxidative stress and mitochondrial dysfunction occur early and often progress with severity of Alzheimer's disease. *J. Alzheimers Dis.* **9,** 167–181
46. Szolnoki, Z., Kondacs, A., Mandi, Y., Bodor, A., and Somogyvari, F. (2009) A homozygous genetic variant of mitochondrial uncoupling protein 4 exerts protection against the occurrence of multiple sclerosis. *Neuromolecular Med.* **11,** 101–105